THE ASTROPHYSICAL JOURNAL, 495:L119–L122, 1998 March 10
© 1998. The American Astronomical Society. All rights reserved. Printed in U.S.A.

THE MILLIMETER AND SUBMILLIMETER ROTATIONAL SPECTRUM OF THE KS RADICAL ($X\ ^2\Pi_i$)

J. XIN AND L. M. ZIURYS
Department of Astronomy and Department of Chemistry, Steward Observatory, University of Arizona, 933 North Cherry Avenue, Tucson, AZ 85721-0065
Received 1997 September 25; accepted 1998 January 7; published 1998 February 27

ABSTRACT

The pure rotational spectrum of the KS radical ($X\ ^2\Pi_i$) has been recorded using millimeter/submillimeter direct absorption techniques in the range 248–409 GHz. This work is the first laboratory detection of KS by any method. The species was created by the reaction of potassium vapor and CS_2 under DC discharge conditions. Twenty-three rotational transitions were measured in both spin-orbit components, $\Omega = 1/2$ and $\Omega = 3/2$; lambda-doubling splittings were resolved in each substate. These data were analyzed with a $^2\Pi$ case (*a*) Hamiltonian, and the rotational, spin-orbit, and lambda-doubling parameters have been determined. The lambda-doubling *p*-constant was found to be anomalously large, indicating the presence of a $^2\Sigma$ state that is close by. The detection of KCl in the circumstellar shell of IRC +10216 indicates that potassium is present in the gas phase and may be in the form of other species such as KS.

Subject headings: ISM: molecules — line: identification — molecular data

1. INTRODUCTION

At the present time, little is known about the abundance and distribution in the dense gas of elements from the fourth row of the periodic table, although several of them have substantial cosmic abundances. For example, some transition metals are quite prevalent, including iron (Fe/H $\sim 2.6 \times 10^{-5}$), chromium (Cr/H $\sim 4.0 \times 10^{-7}$), and even nickel (Ni/H $\sim 1.5 \times 10^{-7}$) (e.g., Sharp & Huebner 1990). The only fourth-row element that has been detected to date in dense material is potassium, which has a cosmic abundance of K/H $\sim 1.3 \times 10^{-7}$. It has been observed in one molecule, KCl, toward the circumstellar envelope of the late-type carbon star IRC +10216 (Cernicharo & Guélin 1987).

In diffuse gas, much more is known about gas-phase abundances and the corresponding depletions of the fourth-row elements from optical measurements of atoms against background stars. Such observations suggest that iron, titanium, and calcium are highly depleted relative to their cosmic abundances (e.g., Sofia, Cardelli, & Savage 1994). Potassium, on the other hand, undergoes only moderate depletion.

In contrast, with the exception of argon, all third-row elements have been detected in molecules in either dense clouds or circumstellar envelopes. For example, chlorine (Cl/H $\sim 1.8 \times 10^{-7}$) has been observed in the form of HCl toward SgrB2 and Orion (e.g., Zmuidzinas et al. 1995). Phosphorus, which has a cosmic abundance of 3.0×10^{-7}, has been detected in the PN and CP molecules (e.g., Ziurys 1987; Guélin et al. 1990). Certain metal-bearing species have been observed in the shell of IRC +10216, including MgNC, MgCN, AlCl, AlF, NaCN, and NaCl (Guélin, Lucas, & Neri 1996). Therefore, detection of molecules containing fourth-row elements may not be unexpected.

High spatial resolution maps of IRC +10216 carried out with the Plateau de Bure interferometer indicate that emission from NaCl and AlCl is confined to the inner envelope, extending no more than 10″ from the central star (e.g., Guélin et al. 1996). Although such mapping has not yet been carried out for KCl, this molecule is likely to have a similar distribution to the other chloride species. However, the carriers of potassium in the outer envelope of IRC +10216 are unknown. One problem in studying this element has been the lack of accurate rest frequencies for K-containing molecules. With the exception of a few species such as KOH (Kuczkowski, Lide, & Krisher 1966) and KCN (Törring et al. 1980), as well as the halides, few simple potassium-bearing molecules have been studied by high-resolution spectroscopy.

In this Letter, we present the first laboratory detection of KS and the measurement of its pure rotational spectrum. This free radical was found to have a $^2\Pi_i$ ground state, similar to NaS (Li & Ziurys 1997). Rotational transitions were recorded for both the $\Omega = 3/2$ and $\Omega = 1/2$ spin-orbit components of KS in the range 248–409 GHz. Along with the rest frequencies, rotational, spin-orbit, and lambda-doubling parameters of this species have been determined.

2. EXPERIMENTAL

The transition frequencies of KS were recorded using one of the millimeter/submillimeter spectrometers of the Ziurys group (Ziurys et al. 1994). Briefly, the instrument consists of a phase-locked Gunn oscillator/Schottky diode multiplier source, a double-pass reaction chamber incorporating a Broida-type oven, and a helium-cooled InSb detector. The optics of the spectrometer were designed using Gaussian-beam methods. The source is modulated to enable phase-sensitive detection, and all signals are processed at 2*f* such that second-derivative spectra are measured.

The KS radical was created by the reaction of potassium vapor and carbon disulfide (CS_2) under DC discharge conditions. The vapor was produced in the Broida-type oven and entrained in 20 mtorr of argon carrier gas. About 5 mtorr of CS_2 was added to this mixture and discharged using a current of 50 mA at 200 V. The reaction plasma glowed bright purple, presumably from atomic potassium emission.

Transition frequencies were measured for 92 separate lines of KS. Frequencies were determined from Gaussian fits to the line profiles, obtained from an average of two 5 MHz wide scans, one in increasing frequency and the other in decreasing frequency. Line widths were 600–700 kHz over the 248–409 GHz range. Experimental accuracy is estimated to be ± 100 kHz.

TABLE 1

OBSERVED TRANSITION FREQUENCIES OF KS ($X\ ^2\Pi_i$)[a]

		$^2\Pi_{3/2}$		$^2\Pi_{1/2}$	
$J'' \rightarrow J'$	PARITY	ν_{obs}	$\nu_{obs} - \nu_{calc}$	ν_{obs}	$\nu_{obs} - \nu_{calc}$
33.5 → 34.5	*e*	249430.995	−0.058	248813.650	−0.004
	f	249434.792	−0.072	251050.353	−0.017
34.5 → 35.5	*e*	256628.685	−0.014	256027.073	−0.048
	f	256632.710	−0.021	258260.441	0.008
35.5 → 36.5	*e*	263823.565	−0.018	263237.821	0.002
	f	263827.815	−0.025	265467.641	−0.032
36.5 → 37.5	*e*	271015.615	−0.012	270445.691	0.020
	f	271020.098	−0.017	272671.996	−0.011
37.5 → 38.5	*e*	278204.736	−0.019	277650.634	−0.010
	f	278209.462	−0.019	279873.292	−0.015
38.5 → 39.5	*e*	285390.870	−0.019	284852.628	0.018
	f	285395.856	−0.001	287071.642	0.098
39.5 → 40.5	*e*	292573.942	−0.006	292051.527	0.008
	f	292579.155	−0.010	294266.600	−0.017
40.5 → 41.5	*e*	299753.862	0.003	299247.294	0.030
	f	299759.322	−0.009	301458.443	−0.024
41.5 → 42.5	*e*	306930.552	0.010	306439.813	0.006
	f	306936.262	−0.011	308646.950	−0.028
42.5 → 43.5	*e*	314103.957	0.037	313629.043	0.007
	f	314109.951	0.035	315832.109	0.006
43.5 → 44.5	*e*	321273.940	0.027	320814.894	0.025
	f	321280.215	0.035	323013.850	0.078
44.5 → 45.5	*e*	328440.460	0.014	327997.240	−0.001
	f	328447.012	0.023	330191.901	0.014
45.5 → 46.5	*e*	335603.482	0.042	335176.077	−0.009
	f	335610.306	0.041	337366.354	−0.002
46.5 → 47.5	*e*	342762.840	0.021	342351.235	−0.038
	f	342769.971	0.041	344537.116	−0.038
47.5 → 48.5	*e*	349918.528	0.026	349522.774	−0.033
	f	349925.933	0.028	351704.133	0.013
48.5 → 49.5	*e*	357070.424	0.008	356690.518	0.009
	f	357078.151	0.035	358867.224	−0.048
49.5 → 50.5	*e*	364218.495	0.018	363854.400	0.017
	f	364226.496	0.017	366026.462	0.007
50.5 → 51.5	*e*	371362.641	0.026	371014.321	0.003
	f	371370.947	0.022	373181.622	0.013
51.5 → 52.5	*e*	378502.729	−0.016	378170.173	−0.040
	f	378511.373	0.006	380332.702	0.008
52.5 → 53.5	*e*	385638.776	−0.019	385322.044	0.025
	f	385647.736	0.002	387479.579	−0.009
53.5 → 54.5	*e*	392770.712	0.026	392469.658	0.004
	f	392779.933	−0.014	394622.210	−0.010
54.5 → 55.5	*e*	399898.301	−0.031	399613.031	0.009
	f	399907.874	−0.046	401760.501	−0.040
55.5 → 56.5	*e*	407021.613	−0.058	406752.031	−0.003
	f	407031.530	−0.061	408894.501	0.048

[a] In units of megahertz.

3. RESULTS AND ANALYSIS

Twenty-three transitions were measured for KS in both spin-orbit ladders, as shown in Table 1. In every transition, lambda-doubling was observed, indicated by *e* and *f* parity designations. For the lower spin-orbit component, $\Omega = 3/2$, the lambda-doubling is small, typically 4–10 MHz, and becomes larger with an increasing J quantum number. For the $\Omega = 1/2$ substate, the doubling is much greater, ranging from 2.14 to 2.24 GHz and decreasing in magnitude with increasing J. This splitting is unusually large and comparable to what is observed in NaO (Yamada, Fujitake, & Hirota 1989). Although potassium 39, the main isotope, has a nuclear spin of 3/2, no evidence of hyperfine interactions was observed in the data, as expected at the high-J levels observed.

Figure 1 displays the $J = 54.5 \rightarrow 55.5$ transition of KS near 400 GHz. The bottom spectrum in the figure shows the lambda doublets originating from the $\Omega = 3/2$ ladder; these lambda doublets are separated by 10 MHz. In the top spectrum, the lambda doublets from the $\Omega = 1/2$ ladder are presented. Here the separation is much greater (~2.15 GHz), and a large frequency gap occurs in the spectrum. The $\Omega = 3/2$ data were taken in a single 50 s scan covering 100 MHz; the $\Omega = 1/2$ spectrum is a truncated composite of two separate 50 s, 100 MHz scans. It should be noted that the intensity scale in the two spectra are arbitrary, but the signal-to-noise ratio is much better for the $\Omega = 3/2$ data.

The data were analyzed using a $^2\Pi$ effective Hamiltonian in a case (*a*) basis of the form

$$\hat{\boldsymbol{H}}_{\rm eff} = \hat{\boldsymbol{H}}_{\rm ROT} + \hat{\boldsymbol{H}}_{\rm CD} + \hat{\boldsymbol{H}}_{\rm SO} + \hat{\boldsymbol{H}}_{\rm SOCD} + \hat{\boldsymbol{H}}_{\rm LD}. \quad (1)$$

In this equation, the first two terms refer to molecular frame rotation and its centrifugal distortion, described by constants B and D. The next two symbols designate the spin-orbit interaction and its centrifugal distortion, corresponding to parameters A, A_D, and A_H. Matrix elements for these interactions

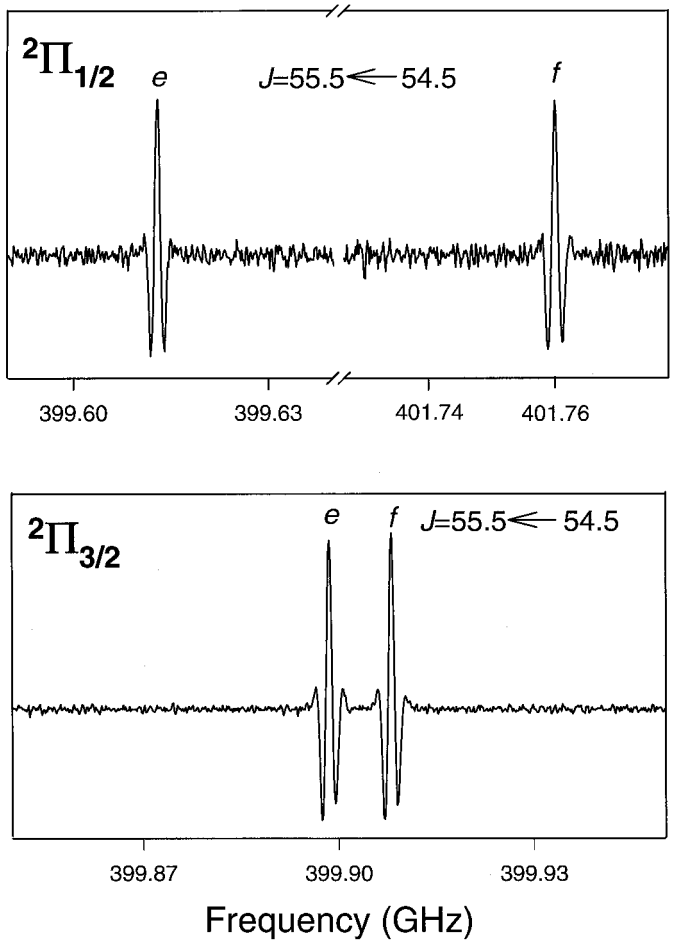


FIG. 1.—Spectrum of the $J = 54.5 \rightarrow 55.5$ transition of KS ($X\ ^2\Pi_i$) observed in this work near 400 GHz. The bottom panel shows the lower spin-orbit component, $\Omega = 3/2$, which consists of two lines, labeled by *e* and *f*, arising from lambda-doubling interactions. The top panel shows the $\Omega = 1/2$ sublevel data, which also consists of lambda-doublets. These doublets, however, are split by over 2 GHz, and hence there is a large frequency gap in the spectrum.

are given in Hirota (1985). The lambda-doubling Hamiltonian used in this case is

$$\hat{\boldsymbol{H}}_{\rm LD} = 1/2\,(p + 2q)\,(\boldsymbol{J}_+\boldsymbol{S}_+ + \boldsymbol{J}_-\boldsymbol{S}_-) - 1/2q\,(\boldsymbol{J}_+^2 + \boldsymbol{J}_-^2)\,, \quad (2)$$

where p and q are the lambda-doubling parameters defined by Brown et al. (1978), which are basically the Mulliken & Christy (1931) definitions. Centrifugal distortion corrections p_D, q_D, and p_H (but not q_H) had to be added to the lambda-doubling Hamiltonian in order to obtain an acceptable fit. Such corrections are justified, given the high-J levels involved in the analysis and the large lambda-doubling in the $\Omega = 1/2$ component. The centrifugal distortion term has the form (see Brown et al. 1978)

$$\begin{aligned}\hat{\boldsymbol{H}}_{\rm CDLD} = {} & 1/4(p_D + 2q_D)[(\boldsymbol{J}_+\boldsymbol{S}_+ + \boldsymbol{J}_-\boldsymbol{S}_-)\boldsymbol{R}^2 \\ & + \boldsymbol{R}^2(\boldsymbol{J}_+\boldsymbol{S}_+ + \boldsymbol{J}_-\boldsymbol{S}_-)] \\ & - 1/4q_D[(\boldsymbol{J}_+^2 + \boldsymbol{J}_-^2)\boldsymbol{R}^2 + \boldsymbol{R}^2(\boldsymbol{J}_+^2 + \boldsymbol{J}_-^2)] \\ & + 1/4(p_H + 2q_H)[(\boldsymbol{J}_+\boldsymbol{S}_+ + \boldsymbol{J}_-\boldsymbol{S}_-)\boldsymbol{R}^4 \\ & + \boldsymbol{R}^4(\boldsymbol{J}_+\boldsymbol{S}_+ + \boldsymbol{J}_-\boldsymbol{S}_-)] - 1/4q_H[(\boldsymbol{J}_+^2 + \boldsymbol{J}_-^2)\boldsymbol{R}^4 \\ & + \boldsymbol{R}^4(\boldsymbol{J}_+^2 + \boldsymbol{J}_-^2)]. \quad (3)\end{aligned}$$

Because only high-J levels are involved in the data, the spin-orbit constant A is somewhat insensitive to the fit, unlike the situation for NaS (Li & Ziurys 1997). Thus, the A-value was first estimated from the atomic S^- spin-orbit constant ζ in a p^5 configuration, i.e., $A \cong -\zeta_s - (p^5) = -9.8 \times 10^6$ MHz. This value was initially used in the fit. A and A_D are highly correlated, however, and so the fit was carried out by fixing one parameter and changing the other, and vice versa, until both parameters remained invariant.

The spectroscopic parameters determined from this analysis are listed in Table 2. The rms of this fit is 28 kHz. Unfortunately, there are no other constants for KS available from the literature. Therefore, spectroscopic parameters for NaS are used for comparison and are also listed in Table 2. The rotational constants for KS are generally consistent with those of NaS, i.e., smaller constants for a heavier molecule. Also, to a first approximation, p defines the lambda-doubling splitting in the $\Omega = 1/2$ levels, and q in the $\Omega = 3/2$ levels. The magnitude of these constants certainly correlates with the observed doublet splittings.

TABLE 2

SPECTROSCOPIC CONSTANTS FOR KS ($X\ ^2\Pi_i$)[a]

Parameter	KS	NaS[b]
A	−9,000,000(2600)	−8,005,000(7700)
A_D	−4.43476(82)	−0.2750(88)
A_H	0.00003365(17)	0.0001883(57)
B	3626.34752(41)	6100.797(20)
D	0.003260819(87)	0.009169(29)
$H \times 10^8$	...	−2.7(1.3)
p	2296.19(27)	1956.0(2.0)
p_D	−0.015156(67)	−0.0149(15)
$p_H \times 10^6$	0.0000253(37)	−0.002621(24)
q	−0.875(16)	−0.835(43)
$q_D \times 10^6$	4.2(5.5)	...
rms of fit	0.029	0.100

[a] In units of megahertz; errors are 3 σ and apply to the last quoted decimal places.

[b] Revised fit using data of Li & Ziurys 1997 (see text).

4. DISCUSSION

This study securely identifies the ground state of KS to be $X\ ^2\Pi_i$. This identification is based on the presence of lambda-doubling interactions in the spectra and the detection of both spin-orbit components. The ground state must also be inverted because the lines from the substate with the smaller lambda-doubling splitting ($\Omega = 3/2$) have stronger intensities. (To first order, there is no lambda-doubling in the $\Omega = 3/2$ component but only in the $\Omega = 1/2$ levels.) Although NaS also has a $^2\Pi_i$ ground electronic state, it is not certain that KS would as well. Studies of the alkali monoxides have shown that while LiO and NaO have $^2\Pi_i$ ground states (e.g., Freund et al. 1972; Yamada et al. 1989), those of RbO and CsO are $^2\Sigma$ (e.g., Lindsay, Herschbach, & Kwiram 1976). At some point down the alkali column, the $^2\Sigma$ state overtakes the $^2\Pi$ term in energy. Only very limited infrared and electron spin resonance data exist for KO (e.g., Spiker & Andrews 1973), so its ground state is uncertain. Theoretical calculations by Allison, Cave, & Goddard (1984) predict a change in symmetry at RbO for the oxide series, suggesting a $^2\Pi$ ground state for KO, but more recent computations by Langhoff, Partridge, & Bauschlicher (1991) indicate that it may actually be $^2\Sigma$. Such theoretical studies have not been carried out for the alkali sulfide group. The

change in symmetry occurs because of a Pauli repulsion term that becomes important at larger internuclear distances; hence, the $^2\Sigma$ state may be favored even earlier in the alkali series for the sulfides than the oxides. Our study shows quite the reverse effect.

Because the ground states shift from $^2\Pi$ to $^2\Sigma$ with the later alkali metals, it is expected that the nearest $^2\Sigma$-excited state for KS lies closer in energy than that for NaS. In fact, if the pure precession model is assumed (see Mulliken & Christy 1931), the energy difference between the $^2\Pi$ and $^2\Sigma$ states can be estimated from the p-parameter using the following expression:

$$p = \frac{4AB}{E_\Pi - E_\Sigma}. \quad (4)$$

Taking the constants from Table 2, $E_\Sigma - E_\Pi$ is calculated to be about 1900 cm^{-1} for KS, as opposed to 3300 cm^{-1} for NaS. Another result from pure precession is that $q \approx (B/A)p$. Using this relationship, q should be on the order of -0.93 MHz, which is in excellent agreement, both in sign and magnitude, with the fitted value of $-0.875(16)$ MHz. The electron configuration of KS is K$(3s\sigma)^2(3p\sigma)^2(3p\pi)^3$; hence, the lowest lying $^2\Sigma$ state should result from the promotion of a $p\sigma$ electron to a $p\pi$ orbital. Consequently, pure precession should be a reasonable first approximation for describing the lambda-doubling in KS.

The sign of lambda-doubling constant $q(<0)$ of KS differs from that of NaO and NaS, which have $q > 0$. Changing the sign of q reverses the e and f parity assignments, which cannot be determined from pure rotational spectrum. We have subsequently reanalyzed both the NaS and NaO data sets and have obtained very good fits with $q < 0$. The results of the revised fit for NaS are given in Table 2. These details will be further discussed in a later paper.

Another check on the validity of the lambda-doubling parameters is to estimate the value of p_D and q_D. These constants can be calculated from the following formulas (Brown, Carrington, & Sears 1979):

$$p_D \simeq \frac{-2Dp}{B}; \quad q_D \simeq \frac{-4Dq}{B}. \quad (5)$$

From the equations, p_D is estimated to be -0.004 MHz and $q_D \approx 3.2 \times 10^{-6}$ MHz, as opposed to the fitted parameters $p_D = -0.015$ MHz and $q_D = 4.2 \times 10^{-6}$ MHz. These numbers agree to within a factor of 3.5. Consequently, p_D and q_D derived in the analysis appear reasonable.

From the rotational constant, an r_0 bond length for KS can be estimated. This value was calculated to be $r_0 = 2.817$ Å. In contrast, that of NaS is $r_0 = 2.488$ Å. The larger bond length in KS is primarily due to the larger potassium nucleus because the bonding in both sulfide species should be similar.

It is likely that other potassium-bearing species will be present in IRC +10216, if not additional sources, given the detection of KCl. KS is an interesting possibility. Clearly a search for this molecule is warranted and could produce some enlightening results for circumstellar metal chemistry.

This research is supported by NSF grant AST-95-03274 and NASA grants NAGW-2989 and NAG5-3785.

REFERENCES

Allison, J. N., Cave, R. J., & Goddard, W. A., III. 1984, J. Phys. Chem., 88, 1262
Brown, J. M., Carrington, A., & Sears, T. J. 1979, Mol. Phys., 37, 1837
Brown, J. M., Kaise, M., Kerr, C. M. L., & Milton, D. J. 1978, Mol. Phys., 36, 553
Cernicharo, J., & Guélin, M. 1987, A&A, 183, L10
Freund, S., Herbst, E., Mariella, R., & Klemperer, W. 1972, J. Chem. Phys., 56, 1467
Guélin, M., Cernicharo, J., Paubert, G., & Turner, B. E. 1990, A&A, 230, L9
Guélin, M., Lucas, R., & Neri, R. 1996, in IAU Symp. 170, CO: Twenty-five Years of Millimeter-Wave Spectroscopy, ed. W. B. Latter et al. (Dordrecht: Kluwer), 359
Hirota, E. 1985, High Resolution Spectroscopy of Transient Molecules (Berlin: Springer)
Kuczkowski, R. L., Lide, D. R., & Krisher, L. C. 1966, J. Chem. Phys., 44, 3131
Langhoff, S. R., Partridge, H., & Bauschlicher, C. W., Jr. 1991, Chem. Phys, 153, 1
Li, B.-Z., & Ziurys, L. M. 1997, ApJ, 488, L137
Lindsay, D. M., Herschbach, D. R., & Kwiram, A. L. 1976, Mol. Phys., 32, 1199
Mulliken, R. S., & Christy, A. 1931, Phys. Rev., 38, 87
Sharp, C. M., & Huebner, W. F. 1990, ApJS, 72, 417
Sofia, U. J., Cardelli, J. A., & Savage, B. D. 1994, ApJ, 430, 650
Spiker, R. C., Jr., & Andrews, L. 1973, J. Chem. Phys., 58, 713
Törring, T., Bekooy, J. P., Meerts, W. L., Hoeft, J., Tiemann, E., & Dymanus, A. 1980, J. Chem. Phys., 73, 4875
Yamada, C., Fujitake, M., & Hirota, E. 1989, J. Chem. Phys., 90, 3033
Ziurys, L. M. 1987, ApJ, 321, L81
Ziurys, L. M., Barclay, W. L., Jr., Anderson, M. A., Fletcher, D. A., & Lamb, J. W. 1994, Rev. Sci. Instrum., 65, 1517
Zmuidzinas, J., Blake, G. A., Carlstrom, J. E., Keene, J., & Miller, D. 1995, ApJ, 447, L125